



**Abstract**

17

18

19

20

21

22

23

24

25

26

27

28

29

30

31

32

33

34

35

36

37

A conceptual coupled ocean-atmosphere model is used to study coupled ensemble data assimilation schemes with the focus on the role of ocean-atmosphere interaction in the assimilation. The optimal scheme is the fully coupled data assimilation scheme that employs the coupled covariance matrix and assimilates observations in both the atmosphere and ocean. The assimilation of synoptic atmospheric variability that captures the temporal fluctuation of the weather noise is found critical for the estimation of not only the atmospheric, but also oceanic states. The synoptic atmosphere observation is especially important in the mid-latitude system, where oceanic variability is driven by weather noise. The assimilation of synoptic atmospheric variability in the coupled model improves the atmospheric variability in the analysis and the subsequent forecasts, reducing error in the surface forcing and, in turn, in the ocean state. Atmospheric observation can further improve the oceanic state estimation directly through the coupled covariance between the atmosphere and ocean states. Relative to the mid-latitude system, the tropical system is influenced more by ocean-atmosphere interaction and, thus, the assimilation of oceanic observation becomes more important for the estimation of the ocean and atmosphere.

## 38 **1. Introduction**

39 As a flow-dependent data assimilation scheme, Ensemble Kalman Filter (EnKF)  
40 (Evensen, 1994; Tippett et al., 2003) in principle is equivalent to the 4-dimensional  
41 Variational Assimilation (4D-Var) scheme. Yet, EnKF is much more promising for the  
42 application to complex models such as coupled ocean-atmosphere general circulation  
43 models (OAGCMs), because it does not require an adjoint model. In an OAGCM, EnKF  
44 is critical in the model initialization for climate predictions (e.g. Zhang et al., 2009,  
45 2010). Since the memory of the climate system lies in the ocean, most prediction studies  
46 have focused on the improvement of the initial state of the ocean. Previous works for the  
47 initialization in OAGCMs either used crude nudging schemes (e.g. Latif et al., 1993;  
48 Rosati et al., 1997; Luo et al., 2005; Smith et al., 2007; Keenlyside et al., 2008), or  
49 applied data assimilation in the component model separately (e.g. Ji et al., 1995; Rosati et  
50 al., 1997; Fuji et al., 2009). Recently, an EnKF scheme is implemented in an OAGCM  
51 for the assimilation of both atmospheric and oceanic data (Zhang et al., 2007). This  
52 scheme is found to improve the initial coupled state, and in turn, the seasonal climate  
53 prediction, significantly over that from a traditional 3-dimensional Variational  
54 Assimilation (3D-Var) ocean initialization (Zhang et al., 2008). However, except for a  
55 few studies in simplified coupled climate models (e.g. Sun et al., 2002; Zhang et al.,  
56 2011, Zhang, 2011a,b), EnKF has not been explored extensively in coupled climate  
57 models. This is due partly to the relatively new development of the EnKF method itself  
58 and partly to the more complex nature of the coupled climate system, especially the  
59 different time scales between the atmosphere and ocean. Therefore, important issues on  
60 EnKF assimilation in OAGCMs remain to be explored. Here, we are concerned with two

61 questions. First, how important is the assimilation of synoptic atmospheric variability for  
62 coupled climate prediction? Second, what is the role of ocean-atmosphere coupling in  
63 coupled data assimilation and for the initialization and climate prediction?

64         There have been studies that suggest the importance of the assimilation of  
65 atmospheric observations in climate prediction, notably El Nino Southern Oscillation  
66 (ENSO) prediction. Using a simple nudging scheme, forecast is improved using the initial  
67 ocean state that is forced by the observed surface wind (Cane et al., 1986; Latif et al.,  
68 1993), and furthermore, the initialization is obtained by assimilating the observed surface  
69 wind in the coupled mode, instead of forcing the ocean in the ocean-alone mode (Chen et  
70 al., 2002). Using an EnKF, ENSO forecast is improved by including the assimilation of  
71 atmospheric observations in the coupled model, relative to that initialized using the  
72 ocean-alone 3D-VAR assimilation (Zhang et al., 2008). Yet, there have been no studies  
73 that systematically explored the roles of coupled assimilation and atmospheric  
74 observation in the coupled system.

75         Here, we will explore the role of coupled assimilation and the role of atmospheric  
76 observation in coupled EnKF data assimilation systematically. As a pilot study here, we  
77 will apply EAKF (a type of EnKF, Anderson, 2001, 2003) to a simple conceptual coupled  
78 ocean-atmosphere model. We will compare various coupled assimilation schemes with  
79 the focus on the role of ocean-atmosphere coupling in the coupled system. Special  
80 attention is also paid to the role of synoptic atmospheric observations in the coupled  
81 assimilation. The coupled climate will be studied in two settings, a mid-latitude-like  
82 system and a tropical-like system, the former being driven completely by weather noises.  
83 Our study shows that the fully coupled assimilation scheme, which assimilates both

84 oceanic and atmospheric observation through the coupled covariance matrix, gives the  
 85 best analysis. This optimal analysis is achieved because the assimilation of synoptic  
 86 atmospheric variability improves the surface atmospheric forcing to the ocean. In  
 87 particular, high frequency atmospheric data captures the temporal behavior of the weather  
 88 noise and therefore improves the surface “stochastic” atmospheric forcing to the ocean.  
 89 The weather noise forcing is particularly important in the mid-latitude system. In  
 90 addition, the coupled covariance between the atmospheric and oceanic states further  
 91 improves the oceanic state directly in the analysis through the background covariance  
 92 between the atmosphere and ocean.

93 The paper is arranged as follows. We will describe our conceptual coupled  
 94 climate model in section 2. We will then compare different coupled assimilation schemes  
 95 in the mid-latitude and tropical systems in section 3 and 4, respectively. A summary and  
 96 discussion will be given in section 5.

## 97 **2. The Model**

98 The simple climate model consists of a fast and chaotic “atmosphere” and a  
 99 slowly oscillating “ocean”. The atmospheric “wind”, or “weather noise”, is governed by  
 100 the Lorenz63 model (Lorenz, 1963)

$$\begin{aligned}
 & m_1 \frac{dx_1}{dt} = a_1(x_2 - x_1) \\
 101 \quad & m_1 \frac{dx_2}{dt} = b_1 x_1 - x_2 - x_1 x_3 \quad , \\
 & m_1 \frac{dx_3}{dt} = x_1 x_2 - c_1 x_3
 \end{aligned} \tag{1}$$

102 where the factor  $m_l = 1/6$  is used to match the time steps of the Lorenz model with the  
 103 rest of model equations. The “surface air temperature”  $T_a$  is determined by an idealized  
 104 thermodynamic model

$$105 \quad m_a \frac{dT_a}{dt} = c(T - T_a) - \mu_a T_a + c_4 x_2. \quad (2)$$

106 The slow ocean consists of the “sea surface temperature” (SST)  $T$  and “thermocline  
 107 depth”  $h$ , which are described by an oscillator model (Jin, 1997) :

$$108 \quad \begin{aligned} \frac{dT}{dt} &= RT + \gamma h + c(T_a - T) + c_2 x_2 - e_n (h + bT)^3 \\ \frac{dh}{dt} &= -rh - \alpha bT \end{aligned} \quad (3)$$

109 The default model parameters are

$$110 \quad a_l = 10, b_l = 28, c_l = 8/3, m_a = 1/20, \mu_a = 1/3, \quad (4)$$

111 for the atmosphere,

$$112 \quad \alpha = 0.125, \gamma = 0.75, r = 0.25, b_0 = 2.5, \mu = 0.5, b = b_0 \mu, R = \gamma b - 1 = 0.3125, e_n = 1, \quad (5)$$

113 for the ocean,

$$114 \quad c = 1, \quad (6a)$$

115 for thermal coupling, and

$$116 \quad c_2 = 0.05, c_4 = 0.1. \quad (6b)$$

117 for the forcing of weather noise. All variables are in the nondimensional form, with a  
 118 nondimensional time  $t \sim 1$  corresponding to a dimensional time  $\sim 2$  months. The model is  
 119 solved using a 4-th order Runge-Kutta method, with a time step of  $dt = 0.002$  ( $\sim 2.88$  hrs,  
 120 or 250 steps  $\sim 1$  month).

121           In this conceptual coupled model, the Lorenz63 model can be thought to represent  
122 internal atmospheric variability of, say, “wind”; this wind component is induced by the  
123 chaotic instability of the atmosphere itself and is independent of oceanic feedback. The  
124 wind variability acts as a weather noise that drives the air temperature (via the term  $c_4x_2$ )  
125 and SST (via the term  $c_2x_2$ ) variability.<sup>1</sup> The air temperature is coupled with SST  
126 through a negative ocean-atmosphere feedback  $c(T-T_a)$  and thus represents the part of  
127 atmospheric variability that is strongly coupled with the ocean. The ocean model was  
128 originally derived for the tropical coupled ocean-atmosphere system (as the recharge  
129 oscillator model, Jin, 1997) with an internal oscillation mode of  $\sim 2$ -3 years. This  
130 oscillator is used here symbolically to represent an ocean-alone system. To avoid  
131 confusion, this model will be called the ocean oscillator model hereafter.

132           In spite of its simplicity, the conceptual model captures the essential feature of a  
133 coupled system, with a fast atmosphere (days) coupled with a slowly varying ocean  
134 (months to years). The model parameters for the atmosphere wind model (1) and the  
135 oceanic model (3) are the the standard parameters of Lorenz (1963) and Jin (1997),  
136 respectively, except for the tunable relative coupling strength  $\mu$ . Other model parameters  
137 are tuned such that the coupled model captures some important statistical features of the  
138 coupled variability in a much more realistic system (see later discussion on Figs.2 and 4)  
139 such that this model may be of relevance to more complex climate systems. We  
140 constructed two model settings, a mid-latitude-like and a tropics-like coupled systems. In  
141 the mid-latitude system, parameters take the default values in eqns. (4)-(6). In particular,

---

<sup>1</sup> The internal variability “wind” can also be thought as “precipitation”, which forces salinity variability in the ocean but with little feedback from the salinity.

142 the oceanic instability parameter is small ( $\mu=0.5$  in (5)) such that the oceanic mode is a  
143 damped oscillating mode. As such, the mid-latitude system is driven completely by the  
144 atmospheric noise using large forcing parameters  $c_2=0.05$ ,  $c_4=0.1$  in (6b). In the tropical  
145 system, the atmospheric forcing effect is reduced by 10 times to  $c_2=0.005$ ,  $c_4=0.01$ .  
146 Furthermore, the instability is enhanced with  $\mu=1.5$  such that the oceanic mode becomes  
147 self-exciting. Mathematically, the mid-latitude system is a damped system forced by  
148 strong stochastic noise, while the tropical system is a self-exciting system modified by  
149 weak stochastic noise.<sup>2</sup>

150 In the mid-latitude system, the atmospheric wind exhibits fast and chaotic  
151 variability (Fig.1b). The ocean exhibits slow irregular oscillation punctuated by rapid  
152 events associated with the atmospheric forcing (Fig.1a); the air temperature consists of  
153 fast variability due to the wind and slow variability due to SST feedback (Fig.1b). The  
154 mid-latitude system captures some major features in a state-of-art OAGCM, the National  
155 Center for Atmospheric Research Community Climate System Model version 3.5 (NCAR  
156 CCSM3.5), as seen by comparing the lagged correlation in the mid-latitude North  
157 Atlantic in the OAGCM CCSM3.5 (Fig.2a) and in the simple model (Fig.2b). In the  
158 CCSM3.5 (Fig.2a) and the simple model (Fig.2b), both auto-correlations imply a short  
159 decorrelation time less than a month for the surface wind and a long decorrelation time of  
160 several months for the SST. Both autocorrelations of the air temperature decline rapidly  
161 in the first month and then slowly for several months, both attributed by the fast  
162 atmospheric wind and slow SST feedback. Both cross-correlations between wind and

---

<sup>2</sup> The intensity of noise forcing plays the critical role here. The result remains robust for the mid-latitude system when the instability parameter is increased to  $\mu=1.5$ , and remains robust for the tropical system when the instability parameter is reduced to  $\mu=0.5$ .

163 SST are higher for wind leading SST than for SST leading wind, suggesting that the wind  
164 is a major driving agent for SST variability with little feedback from SST. In comparison,  
165 both cross-correlations between air temperature and SST are more symmetric with lead-  
166 lags, although the correlations are still stronger for air temperature leading SST. This  
167 reflects the nature of the negative ocean-atmosphere feedback in the mid-latitude, with  
168 the air-sea heat flux playing a dual role of first driving and later damping the SST  
169 (Frankignoul et al., 1998). Therefore, the simple model captures some statistical features  
170 of ocean-atmosphere feedback in more realistic systems.

171 In the tropics, the ocean exhibits a self-exciting oscillation without any  
172 perturbation. Fig.3a and b show a self-exciting solution perturbed weakly by the chaotic  
173 atmosphere. In comparison with the mid-latitude in Figs.1a, b, the tropical solution  
174 exhibits a much more regular cycle perturbed by weak noise. Due to the weak impact of  
175 weather noise, the lagged correlation shows that, in both the OAGCM (meridional wind,  
176 Fig.4a) and the simple model (Fig.4b), the air temperature almost co-vary with SST,  
177 while the wind is almost uncorrelated with SST.

178 In short, in spite of its idealized nature, the simple model captures important  
179 features of the coupled ocean-atmosphere system and therefore provides a useful tool for  
180 exploring the role of ocean-atmosphere interaction in coupled assimilation.

### 181 **3. Coupled Assimilation in the Mid-latitude System**

182 We now study different schemes of data assimilation in the coupled mid-latitude  
183 model in the perfect model scenario, with the focus on the ocean state, whose long  
184 memory is critical for climate predictability. First, a control simulation is performed with  
185 the initial condition  $h=0$ ,  $T=0$ ,  $T_a=0.15$ ,  $x_1=x_2=x_3=0.0001$  (Figs.1, 3). The model is spun

186 off and then integrated for 200 yrs to represent the “truth”. A synthetic observation is  
187 constructed by adding an observational noise onto the truth. The observational error for  
188 each variable is an independent Gaussian noise with a standard deviation 10% that of the  
189 control simulation. Unless otherwise specified, the coupled model assimilates the  
190 observation every 10 steps (~1.2 days) for the atmosphere and 40 steps (~5 days) for the  
191 ocean. Each ensemble has 20 members and each assimilation is integrated for 200 years  
192 with no inflation on the background covariance. The initial condition for the ensemble  
193 member is constructed from the observation at the time with a small random perturbation.  
194 Here, we discuss the results with all observational variables assimilated. When a subset  
195 of the observational states are assimilated, the results remain qualitatively consistent.  
196 Further sensitivity experiments show that our major conclusion remains qualitatively  
197 valid for other settings, including assimilation time steps, ensemble members, the  
198 magnitude of the observational error and the inflation factors.

199 We first compare three coupled assimilation schemes in the mid-latitude system,  
200 all using the coupled background covariance matrix in the filter analysis: CP-A  
201 assimilates the atmospheric observation only, CP-O assimilates the oceanic observation  
202 only, and CP-AO assimilates both atmospheric and oceanic observations (Table 1). We  
203 will compare the results of these schemes in terms of the normalized RMSEs (root mean  
204 square error normalized by the standard deviation of the control)<sup>3</sup>. The most  
205 comprehensive scheme is the fully coupled assimilation scheme CP-AO, which  
206 assimilates observations of both the atmosphere and ocean. The RMSE is reduced to 30%

---

<sup>3</sup> To reduce the impact of the outlier problem in EAKF (Lawson and Hansen, 2004; Anderson, 2010; Liu et al., 2012), a simple approach is used here: for each scheme, the RMSE is calculated with the top 5% of the RMSEs excluded (the result is similar if the top 1% is excluded). This way, our major conclusions become robust for different assimilation settings and model parameters.

207 (~0.03) and 3% (~0.003) of the observational errors for the atmosphere and ocean,  
208 respectively (Fig.5). (note, in Fig.5, the uncoupled scheme As-O will be discussed later in  
209 section 3b). If only the ocean observation is assimilated (CP-O), the RMSE is reduced to  
210 20% (~0.02) and 85% (~0.085) of the observational errors for  $h$  and SST, respectively  
211 (Fig.5), but remains comparable with the control for the atmospheric variables, with the  
212 RMSEs of 0.55 and  $0.9^4$  (both off scale in Fig.5) for air temperature and winds,  
213 respectively. The modest oceanic errors, especially for SST, are much larger than those in  
214 CP-AO, suggesting the importance of the atmospheric observation for the ocean state in  
215 the coupled assimilation. The poor constrain of the ocean observation on the atmosphere  
216 is expected because the wind does not respond to SST (as in eqn. (1), and the poor  
217 correlation  $< 0.2$ , Fig.A1b), and the air temperature is driven primarily by the stochastic  
218 wind forcing with only a weak response to SST (correlation  $< 0.4$ , Fig.A1b).

219 In contrast, when the atmospheric observation is assimilated into the coupled  
220 model (CP-A), the analysis is improved dramatically. The RMSE of CP-A is reduced to  
221 almost the same level as in CP-AO (Fig.5). This suggests that, for the mid-latitude  
222 system, atmospheric observation can play a much more important role than the oceanic  
223 observation for the coupled state. It is interesting that the atmospheric observation is even  
224 more important than the oceanic observation itself for the ocean state. The critical  
225 importance of the atmospheric observation here can be understood, partly, from the  
226 dynamic nature of the mid-latitude coupled system. The SST variability is forced by  
227 synoptic atmospheric variability, which is often considered as stochastic noise at the slow

---

<sup>4</sup> Even though the atmospheric wind is forcing the air temperature and SST dynamically, with no dynamic feedback at all as shown in eqn. (1), the wind is still improved slightly by oceanic observations (normalized RMSE below 1 in CP-O). Our further experiments show that this improvement is due to the background covariance between the wind and air temperature used in the analysis. Therefore, SST observation improves the air temperature, and in turn, wind. The instantaneous covariance allows the “response” variable to improve the “forcing” variable.

228 ocean (and climate) time scale (Frankignoul and Hasselmann, 1977). This dominant role  
229 of atmospheric forcing on SST is shown clearly in the lagged correlation between SST  
230 and air temperature (Fig.A1f), where the maximum correlation ( $\sim 0.6$ ) occurs when air  
231 temperature leads SST (by  $\sim 80$  steps). Therefore, as synoptic atmospheric forcing is  
232 improved, the ocean state is also improved.

### 233 a) The role of synoptic atmospheric forcing

234 We now further explore the role of synoptic atmospheric observation on the  
235 coupled assimilation. As atmospheric observation becomes less frequent, we speculate  
236 that the effect of the atmospheric observation on the coupled, in particularly the oceanic,  
237 state, will be reduced. Less frequent atmospheric observation should increase the analysis  
238 error in both CP-A and CP-AO and, furthermore, the error will increase faster in CP-A  
239 than in CP-AO because the latter is constrained by the ocean observation. This  
240 speculation is confirmed by two sets of assimilation experiments in CP-A and CP-AO, in  
241 which the atmospheric observational steps are increased from 10 to 640 steps  
242 systematically (while the ocean observation remains fixed at 40 steps). Fig.6 shows the  
243 RMSE ratio between the CP-A and CP-AO experiments as a function of the atmospheric  
244 assimilation steps. Since ocean variability is forced by the entire history of the  
245 atmospheric forcing, as a measure of the error of the atmospheric forcing, the RMSEs  
246 here are accumulated over both analysis and forecast steps<sup>5</sup>. Overall, as the steps of the  
247 atmospheric observation increase, the RMSE ratio tend to increase for the ocean (Fig.6a)  
248 and air temperature (Fig.6b), indicating a faster increase of RMSE in CP-A than in CP-  
249 AO. Therefore, ocean observations become more important for the ocean and air

---

<sup>5</sup> The variation of the RMSE ratio also remains similar for the analysis RMSEs (not shown).

250 temperature as atmospheric observations become less frequent. (The ratio of RMSEs for  
251 wind remains  $\sim 1$  (not shown) because of the lack of oceanic impact on wind). In Fig.6b,  
252 the RMSE ratio for air temperature increases from 1 (at step 10) to 1.15 (at step 640) (the  
253 slight decreases at steps 20 and 80 are likely caused by sampling error). Therefore, the  
254 RMSE of air temperature increases slightly faster in CP-A than in CP-AO, reflecting the  
255 weak impact of SST on air temperature (Fig.6b). The faster error growth in the  
256 atmospheric forcing then leads to a faster error growth in the ocean in CP-A than in CP-  
257 AO, and the RMSE ratios for oceanic variables increase eventually much beyond 1 for  
258 large atmospheric observational steps (Fig.6a). Indeed, in the limit of very large  
259 atmospheric observational steps, the RMSE of oceanic variability in CP-A saturates  
260 towards the control ( $\sim 60\%$  of control at step 640, not shown) because the CP-A scheme  
261 now uses virtually no observations in the atmosphere and ocean; the RMSE of oceanic  
262 variability in CP-AO, however, saturates towards that of CP-O (about 5%-10% of the  
263 control at step 640, not shown), because CP-AO now still uses full oceanic observations  
264 (every 40 steps). Since the RMSE of the ocean is much larger in CP-A than in CP-O, the  
265 RMSE ratio between CP-A and CP-AO grows very large in the ocean, especially for  $h$ .

266 In spite of this overall increase trend of the RMSE ratio, it is important to note  
267 that the RMSE ratio remains close to  $\sim 1$  for air temperature (Fig.6b) and ocean (Fig.6a)  
268 for sufficiently high frequency of atmospheric observations, notably at steps 10, 20 and  
269 even 40. This occurs because the atmospheric observation is so frequent that the forecast  
270 error has not grown significantly in the atmosphere, therefore, the error of the  
271 atmospheric forcing is not much larger in CP-A than in CP-AO (as seen in the RMSE  
272 ratio of air temperature in Fig.6b). The atmospheric forcing is therefore sufficiently

273 accurate in CP-A such that the addition of oceanic observations in CP-AO does not  
274 improve the ocean state significantly (Fig.6a). This argument also implies that the  
275 critical frequency of atmospheric observation should be significantly shorter than the  
276 saturation time of forecast error, or crudely the persistence time. The atmospheric  
277 decorrelation time is less than ~40 steps for wind (Figs.A1c-e), and less than ~150 steps  
278 for air temperature (using a cut off correlation of ~0.2). Therefore, the critical frequency  
279 beyond which the RMSE ratio increases above 1 should be shorter than ~40 – 150 steps,  
280 consistent with the ~40 steps in Fig.6a. In short, if the atmospheric observation is  
281 sufficiently shorter than its persistence time, the atmospheric observation is able to  
282 improve the atmospheric forcing and, in turn, the oceanic variability, significantly, in the  
283 coupled system.

#### 284 **b) Coupled vs. uncoupled assimilation schemes**

285 We now compare the fully coupled scheme against an uncoupled assimilation  
286 scheme As-O (Table 1). The As-O scheme assimilates both atmospheric and oceanic  
287 observations, but separately in a two-tier approach: first, the atmospheric observation is  
288 assimilated in the atmosphere model forced by the SST observation (Specifically, the  
289 SST forcing at each step is derived from the SSTs at the observational steps using a linear  
290 interpolation). Second, the atmospheric forcing (at analysis and forecast steps) is used to  
291 force the ocean model in its assimilation of oceanic observations. The atmospheric  
292 analysis here is equivalent to the standard atmospheric reanalysis product. For the  
293 oceanic state, the As-O scheme is equivalent to an ocean data assimilation forced by an  
294 atmospheric reanalysis product. In a sense, As-O is similar to many previous works for  
295 the initialization of the ocean state for climate predictions in coupled climate models (e.g.

296 Cane et al., 1986; Latif et al., 1993; Rosati et al., 1997) (although the assimilation  
297 schemes there are not ensemble filters). A comparison of the RMSEs in As-O and CP-  
298 AO (Fig.5) shows that, even with the same atmospheric and oceanic observations, the  
299 RMSE is significantly higher in As-O than in CP-AO, especially for the ocean. The  
300 improved analysis in CP-AO over As-O is due, partly, to the improvement of the SST  
301 forcing (to the atmosphere) through the coupled dynamics. Indeed, the RMSE of the SST  
302 analysis in CP-AO is reduced from the observational error ( $\sim 0.1$ , Fig.5) (which is the  
303 error for the SST forcing in As-O) to less than 5% of the observational error ( $< 0.005$ ,  
304 Fig.5). Relative to As-O, the improved SST forcing CP-AO improves the atmosphere  
305 dynamically, which then improves the ocean dynamically. Indeed, even with the  
306 additional assimilation of oceanic observations, the analysis of As-O is significantly  
307 poorer than that in the coupled scheme CP-A for the ocean state and air temperature  
308 (Fig.5), even though the latter only assimilates the atmospheric observation. This is  
309 consistent with the critical importance of synoptic atmospheric observations as discussed  
310 in Fig.6.

311 To further evaluate the role of atmospheric surface forcing, we performed another  
312 uncoupled oceanic assimilation (not shown) that is the same as As-O except that the  
313 atmospheric forcing is replaced by that in CP-AO at every time step. The RMSE in the  
314 ocean is now reduced by about half of that in As-O (due to the improved atmospheric  
315 forcing), but the RMSE still remains significantly higher than in CP-AO, even though  
316 both ocean assimilations used the same atmospheric forcing. This implies that the  
317 improved surface atmospheric forcing through the coupled dynamics is not the only cause

318 for the improved assimilation in the coupled scheme CP-AO over the uncoupled scheme  
 319 As-O.

### 320 c) The role of coupled background covariance

321 In principle, ocean-atmosphere coupling affects the coupled data assimilation not  
 322 only through the coupled dynamics, but also through the coupled covariance in the filter  
 323 analysis. To further explore the difference between the coupled and uncoupled schemes,  
 324 especially the role of the ocean-atmosphere interaction through the coupled covariance,  
 325 we further compare the fully coupled scheme CP-AO with another coupled scheme: the  
 326 dynamically coupled scheme CP-ABOB (Table 1). In CP-ABOB, atmospheric and  
 327 oceanic observations are assimilated as in CP-AO except that the background covariance  
 328 matrices for the atmosphere and ocean only use the sub-matrices for each component  
 329 separately. Specifically, denote the transposes for atmospheric and oceanic variables as

330  $\mathbf{A} = [x_1, x_2, x_3, T_a]^T$  and  $\mathbf{O} = [T, h]^T$ , respectively, the background covariance matrix is

$$331 \quad \mathbf{B} = \begin{bmatrix} \mathbf{B}_{AA} & \mathbf{B}_{AO} \\ \mathbf{B}_{AO} & \mathbf{B}_{OO} \end{bmatrix}, \quad (7)$$

332 in CP-AO, but

$$333 \quad \mathbf{B}_{ABOB} = \begin{bmatrix} \mathbf{B}_{AA} & 0 \\ 0 & \mathbf{B}_{OO} \end{bmatrix}. \quad (8)$$

334 in CP-ABOB. Here  $\mathbf{B}_{AA} = \langle \mathbf{A}, \mathbf{A} \rangle$ ,  $\mathbf{B}_{OO} = \langle \mathbf{O}, \mathbf{O} \rangle$ ,  $\mathbf{B}_{AO} = \langle \mathbf{A}, \mathbf{O} \rangle$ .

335 A comparison of CP-ABOB and CP-AO (Fig.7) shows that the RMSEs are  
 336 comparable for the atmosphere, but is significantly greater in CP-ABOB than CP-AO for  
 337 the ocean. Therefore, atmospheric observations can improve the ocean significantly in the  
 338 fully coupled scheme CP-AO directly through the coupled covariance. This improvement

339 is further shown to be caused completely by the impact of the atmospheric observation on  
 340 ocean. This is shown in two additional partially coupled experiments CP-A2OB and CP-  
 341 O2AB, which respectively use the coupling covariance  $\mathbf{B}_{AO}$  on the ocean and  
 342 atmosphere, respectively, with the corresponding background covariance matrices

$$343 \quad \mathbf{B}_{A2OB} = \begin{bmatrix} \mathbf{B}_{AA} & 0 \\ \mathbf{B}_{AO} & \mathbf{B}_{OO} \end{bmatrix}, \quad \mathbf{B}_{O2AB} = \begin{bmatrix} \mathbf{B}_{AA} & \mathbf{B}_{AO} \\ 0 & \mathbf{B}_{OO} \end{bmatrix}. \quad (9)$$

344 Fig.7 shows almost the same RMSEs in CP-A2OB and the fully coupled CP-AO, but  
 345 almost the same RMSEs in CP-O2AB and the dynamically coupled CP-ABOB.  
 346 Therefore, for the mid-latitude system here, the impact of the coupled covariance on the  
 347 coupled analysis is due to the atmospheric impact on ocean, with little oceanic impact on  
 348 the atmosphere.

349 It is also interesting to compare CP-ABOB with the uncoupled scheme As-O.  
 350 Fig.7 shows that the RMSE is smaller in CP-ABOB than in As-O for air temperature,  
 351 thermocline and SST. The error reduction in air temperature confirms that atmospheric  
 352 observations improve the atmosphere state more in the coupled model than in the  
 353 uncoupled atmospheric model, because the SST forcing is improved over the observation  
 354 (used in As-O) by the coupled dynamics in the coupled model. For the ocean state, we  
 355 may attribute the reduced RMSE from CP-ABOB to CP-AO to the coupled covariance,  
 356 and from As-O to CP-ABOB to the improvement of atmospheric forcing in the coupled  
 357 model.

358 In short, high frequency synoptic atmospheric observation improves the coupled  
 359 state significantly because of its improvement on the atmospheric analysis and, in turn,  
 360 the surface forcing to the ocean. The fully coupled assimilation CP-AO improves the

361 ocean significantly over the uncoupled scheme As-O for two reasons: the coupled  
362 dynamics improves the atmospheric forcing by improving the SST forcing to the  
363 atmosphere (from As-O to CP-ABOB), and, the coupled background covariance allows  
364 the atmospheric observation to improve the ocean state through the analysis directly.

#### 365 **4. Coupled Assimilation in the Tropical System**

366 We now discuss the tropical system briefly, in comparison with the mid-latitude  
367 system. We will show that the major conclusions in the mid-latitude system still hold  
368 qualitatively in the tropical system: the fully coupled scheme gives the optimal coupled  
369 state and high frequency synoptic atmospheric observations can improve the ocean state  
370 significantly. Quantitatively, however, the stronger ocean-atmosphere coupling in the  
371 tropics renders synoptic atmospheric observation less important than in the mid-latitude,  
372 while oceanic observations become more important.

373 As in the mid-latitude system (Fig.5), the normalized RMSEs in CP-AO, CP-A  
374 and CP-O (Table 1) a minimum in CP-AO, and almost the same in CP-A and CP-AO.  
375 Therefore, CP-AO is the optimal scheme and synoptic atmospheric observation plays a  
376 dominant role. Meanwhile, the assimilation of the ocean observation in CP-O reduces the  
377 RMSEs by half compared with the mid-latitude system for ocean ( $h$  and  $T$ ,  $\sim 0.01$ ,  $\sim 0.045$   
378 in Fig.8, vs.  $\sim 0.02$  and  $\sim 0.09$  in Fig.5) and air temperature ( $\sim 0.35$  vs.  $\sim 0.65$ , off scale in  
379 Fig.8 and Fig.5), due to the stronger ocean-atmosphere coupling and the weaker weather  
380 noise forcing in the tropical system. Indeed, the stronger ocean-atmosphere coupling can  
381 be seen in the much larger correlation between SST and air temperature in the tropical  
382 ( $\sim 0.9$ , Fig.A2b,f) than in the mid-latitude ( $\sim 0.4$ , Fig.A1b,f) systems. The weaker weather  
383 noise forcing can also be seen in the lagged cross-correlation, which peaks almost

384 simultaneously in the tropical system (Fig.A2f), rather than when the air temperature  
385 leads SST in the mid-latitude system (Fig.A1f). The increased role of oceanic  
386 observations in the tropical system can also be seen the RMSE ratio between CP-A and  
387 CP-AO in Fig.9. Although qualitatively similar to the mid-latitude system (Fig.7), an  
388 increase of atmospheric observational steps increases the RMSE more in CP-A than in  
389 CP-AO, quantitatively, the RMSE ratio increases significantly beyond 1 for ocean  
390 (Fig.9a) and air temperature (Fig.9b) at 20 steps, while it remains close to 1 even till ~40  
391 steps in the mid-latitude system.

392 Coupling also improves the estimation, as in the mid-latitude. The RMSE is  
393 reduced from the uncoupled As-O to the coupled CP-AO (Fig.8), similar to the mid-  
394 latitude system (Fig.5). Quantitatively, the RMSE is reduced by 10 times in the tropical  
395 system (0.06 in As-O to 0.007 in CP-AO), but only by a half in the mid-latitude system  
396 (from 0.022 to 0.013), because of a greater role of ocean-atmosphere coupling in the  
397 tropical system. The coupled covariance also improves the estimation (Fig.10) as in the  
398 mid-latitude (Fig.7), in comparison of the fully coupled CP-AO with the dynamically  
399 coupled CP-ABOB. Quantitatively, however, the improvement is much less than in the  
400 tropics, as the RMSE in CP-ABOB is not much greater than in CP-AO for air  
401 temperature and ocean (Fig.10). Therefore, unlike the mid-latitude, where the coupled  
402 covariance is the major mechanism that improves the coupled over the uncoupled  
403 schemes, the improvement of the atmospheric forcing is the major mechanism that  
404 improves the coupled assimilation in the tropics. This is consistent with a stronger ocean-  
405 atmosphere coupling and, in turn, a stronger feedback of SST on air temperature in the  
406 tropical system.

## 407 **5. Summary and Discussions**

408         We studied several coupled schemes of EAKF in a simple coupled ocean-  
409 atmosphere model in the perfect model scenario, with the focus on the role of ocean-  
410 atmosphere interaction in the assimilation. Our study confirms that the optimal  
411 assimilation scheme is the fully coupled data assimilation scheme that assimilates  
412 observations in both the atmosphere and ocean and that employs the coupled covariance  
413 matrix. It is further found that the assimilation of synoptic atmospheric variability is  
414 critical for the improvement of not only the atmospheric state, but also the oceanic state,  
415 especially in the mid-latitude system, where oceanic variability is driven predominantly  
416 by weather noise. Furthermore, atmospheric observation can also improve the oceanic  
417 state through the coupled covariance, especially in the mid-latitude system. Relative to  
418 the mid-latitude system, the tropical system is influenced more by oceanic dynamics and  
419 ocean-atmosphere interaction. Therefore, the assimilation of oceanic observation  
420 becomes more important. This study suggests that the analysis of the coupled climate  
421 state variables are best derived in the fully coupled model using both the atmospheric and  
422 oceanic observations. Furthermore, synoptic atmospheric observations are critical for the  
423 improvement of the coupled analysis. Finally, coupled covariance between the ocean and  
424 atmosphere should also be employed to achieve the best analysis.

425         The importance of synoptic atmospheric observation for improving the ocean  
426 state has important implication for climate predictions: although the memory of the  
427 climate system lies in the ocean, synoptic atmospheric observations can significantly  
428 improve the ocean initial state and, in turn, climate prediction of slow oceanic variables.  
429 Therefore, the synoptic atmospheric observation alone is able to improve the coupled

430 initial state in a balanced way (in both atmosphere and ocean), which will help improving  
431 climate prediction. We performed ensemble climate prediction experiments initialized by  
432 the coupled state of different assimilation schemes. Since each of our schemes (Table 1)  
433 improves the coupled state in both the atmosphere and ocean in a balanced way, it also  
434 improves the climate prediction of slow ocean state. For example, the RMSE is smaller in  
435 CP-AO than As-O in both the ocean and air temperature (Figs.5, 8), which in turn is  
436 smaller than those in CP-O; accordingly, the climate prediction of  $T$  and  $h$  deteriorate  
437 from CP-AO to As-O and finally to CP-O (not shown). One extreme example of  
438 unbalanced initial condition is the perfect ocean experiment (PO), as being used in some  
439 early studies of experimental decadal climate predictions (Collins et al., 2002). In PO, the  
440 ocean initial condition is the truth, while the atmosphere initial state is selected randomly  
441 from the control. A comparison of the climate prediction (Fig.11) shows that the  
442 prediction of the ocean state eventually becomes much worse in PO than in CP-AO after  
443 a very short lead time when ocean is almost perfect in PO. This occurs because the very  
444 large initial error in the atmosphere in PO quickly drives the ocean away from the truth.

445         It is interesting that the major conclusions of our conceptual model study seem to  
446 be consistent with previous studies in more realistic models. The importance of the  
447 atmospheric observations has been recognized even in the early stage of ENSO  
448 prediction, where less advanced assimilation schemes such as nudging are used for  
449 initialization (e.g. Cane et al., 1986; Latif et al., 1993). These studies found that a better  
450 forecast is achieved using the initial ocean state that is forced by the observed surface  
451 wind and the addition of further oceanic observation may not improve climate prediction  
452 significantly. Our conclusion that the assimilation in the coupled scheme (e.g. CP-A)

453 improves the coupled state than the uncoupled assimilation (e.g. As-O) also appears to be  
454 consistent with Chen et al. (2002). They found that their ENSO prediction is improved if  
455 the initialization is obtained by assimilating the observed surface wind in the coupled  
456 mode, instead of forcing the ocean in the ocean-alone mode. The importance of synoptic  
457 wind for improving climate prediction is consistent with the EAKF study in an OAGCM  
458 (Zhang et al., 2008). This study shows that ENSO forecast is improved using the EAKF  
459 in the coupled model compared with the ocean-alone 3D-VAR assimilation.

460       Much further studies are needed, especially in more realistic models. One  
461 surprising result in our model is the overwhelming importance of synoptic atmospheric  
462 observation, such that the assimilation of synoptic atmospheric observation alone (CP-A)  
463 improves the coupled state almost the same as assimilating additionally oceanic  
464 observations (CP-AO). Equivalently, the assimilation of oceanic observation has little  
465 impact on the atmosphere, even the air temperature, as shown in CP-O. Previous studies  
466 with more realistic models, including OAGCMs show that the assimilation of oceanic  
467 observations in the coupled model can indeed improve the atmospheric state, especially  
468 in the tropics (Ji et al., 1995; Rosati et al., 1997; Luo et al., 2005; Fuji et al., 2009). The  
469 overwhelming role of synoptic atmospheric observation in our study could be related to  
470 the lack of dynamic ocean-atmosphere feedbacks in our idealized model, especially in the  
471 tropics. In a more realistic tropical system, the (zonal) wind anomaly is significantly  
472 correlated with SST, because of the strong dynamic response of the atmosphere to  
473 tropical SST anomaly (Gill, 1980; Lindzen and Nigam, 1987). This zonal wind effect is  
474 absent in our tropical system, which only simulates the meridional wind (Fig.4a) and  
475 therefore lacks the dynamic ocean-atmosphere feedback.

476 **Acknowledgement**

477

478 This work is supported by NSF, Chinese 2012CB955201 and NSFC 41130105. SZ is

479 supported by NOAA.

480

481 **Appendix:** Lagged cross-correlations among model variables

482 To help us understand the nature of the covariance among different model variables, and

483 in turn the ensemble filter analysis, the lagged cross-correlations among different model

484 variables are shown for the mid-latitude system in Fig.A1 and for the tropical system in

485 Fig.A2. See the text for discussions.

486

487

488 **References**

- 489 Anderson, J., 2001: An ensemble adjustment Kalman filter for data assimilation. *Mon.*  
490 *Wea. Rev.*, **129**, 2894-2903
- 491 Anderson, J., 2003: A local least squares framework for ensemble filtering. *Mon. Wea.*  
492 *Rev.*, **131**, 634-642
- 493 Anderson, J., 2010: A non-Gaussian ensemble filter update for data assimilation. *Mon.*  
494 *Wea. Rev.*, **138**, 4186-4198
- 495 Cane, M., S. Zebiak and S. Dolan, 1986: Experimental forecasts of El Nino. *Nature*, **321**,  
496 827-832
- 497 Chen, D., S. Zebiak, A. Busalacchi and M. Cane, 1995: An improved procedure for El  
498 Nino forecasting: implications for predictability. *Science*, **269**, 1699-1702
- 499 Collins, M., 2002: Climate Predictability on Interannual to Decadal Time Scales: The  
500 Initial Value Problem. *Clim. Dyn.* **19**, 671-692.
- 501 Evensen, G., 1994: Sequential data assimilation with a nonlinear quasi-geostrophic model  
502 using Monte Carlo methods to forecast error statistics. *J. Geophys. Res.*, **99**, 1043–  
503 1062.
- 504 Frankignoul C. and K. Hasselmann, 1977: Stochastic climate models. Part II: Application  
505 to sea-surface temperature variability and thermocline variability. *Tellus*, **29**, 284–  
506 305.
- 507 Frankignoul, C, A. Czaja, and B. L’Heveder, 1998: Air–sea feedback in the North  
508 Atlantic and surface boundary conditions for ocean models. *J. Climate*, **11**, 2310–  
509 2324.

- 510 Fuji, Y., T. Nakaegawa, S. Matsumoto, T. Yasuda, G. Yamanaka, and M. Kamachi,  
511 2009: Coupled Climate Simulation by Constraining Ocean Fields in a Coupled  
512 Model with Ocean Data, *J. Climate*, **22**, 5541-5557.
- 513 Gill, A. E., 1980: Some simple solutions for heat-induced tropical circulation. *Quart. J.*  
514 *Roy. Meteor. Soc.*, **106**, 447–462.
- 515 Ji, M., A. Leetmaa and J. Derber, 1995: An ocean analysis system for seasonal to  
516 interannual climate studies. *Mon. Wea. Rev.*, **123**, 460-481
- 517 Jin, F., F., 1997: An equatorial ocean recharge paradigm for ENSO. Part I: A conceptual  
518 model. *J. Atmos. Sci.*, **54**, 811-829
- 519 Keenlyside, N., M. Latif, J. Jungclaus, L. Kornblueh and E. Roeckner, 2008: Advancing  
520 decadal-scale climate prediction in the North Atlantic sector. *Nature*, **453**, 84-887.
- 521 Lawson, G. W. and J. A. Hansen, 2004: Implications of stochastic and deterministic  
522 filters as ensemble-based data assimilation methods in varying regimes of error  
523 growth. *Monthly Weather Review*, **132**, 1966–1981.
- 524 Latif M., A. Sterl, E. Maier-Reimer and M. Junge, 1993: Structure and predictability of  
525 the El Nino/Southern Oscillation phenomenon in a coupled ocean-atmosphere  
526 general circulation model. *J. Climate*, **6**, 700-708
- 527 Lindzen R. S. and S. Nigam, 1987: On the role of sea surface temperature gradients in  
528 forcing low level winds and convergence in the tropics. *J. Atmos. Sci.*, **44**, 2418-  
529 2436.
- 530 Liu, Y., X. Rong, Z. Liu, S. Wu, S. Zhang and R. Jacob, 2012: A random subgrouping  
531 scheme for ensemble square root filter (sEnSQF). *Mon. Wea. Rev.*, submitted.
- 532 Lorenz, E. N., 1963: Deterministic non-periodic flow. *J. Atmos. Sci.*, **20**, 130–141.

- 533 Luo, J.-J., S. Masson, S. Behera, S. Shingu, and T. Yamagata, 2005: Seasonal climate  
534 predictability in a coupled OAGCM using a different approach for ensemble  
535 forecasts. *J. Climate*, **18**, 4474–4497.
- 536 Smith, D., M., S. Cusack, A. W. Colman, C. K. Folland, G. R. Harris and J. M. Murphy,  
537 2007: Improved surface temperature prediction for the coming decade from a global  
538 climate model. *Science*, 317, 796-799.
- 539 Sun C., Z. Hao, M. Ghil and D. Neelin, 2002: Data assimilation for a coupled ocean-  
540 atmosphere model: part I: sequential state estimation. *Mon. Wea. Rev.*, **130**, 1074-  
541 1099
- 542 Tippett, M. K., J. L. Anderson, C. H. Bishop , T. M. Hamill and J. S. Whitaker, 2003:  
543 Ensemble square root filters. *Mon. Wea. Rev.*, **131**, 1485- 1490
- 544 Zhang, S., J. Harrison, A. Rosati and A. Wittenberg, 2007: System design and evaluation  
545 of coupled ensemble data assimilation for global oceanic climate studies. *Mon. Wea.*  
546 *Rev.*, **135**, 3541-3564
- 547 Zhang, S., A. Rosati, M. J. Harrison, R. Gudgel and W. Stern, 2008: GFDL's coupled  
548 ensemble data assimilation system, 1980-2006 coupled reanalysis and its impact on  
549 ENSO forecast. *Preprint WCRP3*, Jan. 27 - Feb. 2, 2008, Tokyo.
- 550 Zhang, S., A. Rosati and M. Harrison, 2009: Detection of multi-decadal oceanic  
551 variability by ocean data assimilation in the context of a "perfect" coupled model. *J.*  
552 *Geophys. Res.*, **114**, C12018, doi:10.1029/2008JC005261.
- 553 Zhang, S., A. Rosati and T. Delworth, 2010: The adequacy of observing systems in  
554 monitoring the Atlantic Meridional Overturning Circulation and North Atlantic  
555 climate. *J. Climate*, **23**, doi:10.1175/2010JCLI3677.1, 5311-5324.

- 556 Zhang, S., 2011a: Impact of observation-optimized model parameters on decadal  
557 predictions: Simulation with a simple pycnocline prediction model. *Geophys. Res.*  
558 *Lett.*, **38**, L02702, doi:10.1029/2010GL046133.
- 559 Zhang, S., 2011b: A study of impacts of coupled model initial shocks and state-Parameter  
560 optimization on climate prediction using a simple pycnocline prediction model. *J.*  
561 *Climate*, **24**, 6210-6226.
- 562 Zhang, S., Z. Liu, A. Rosati and T. Delworth, 2011. A study of enhance parameter  
563 correction with coupled data assimilation for climate estimation and prediction using  
564 a simple coupled model. *Tellus A*, **63**, 10963, DOI: 10.3402/tellusa.v63i0.10963  
565

566 **Table 1: Data Assimilation Schemes**

Name	Atmos obs.	Ocean obs.	Model	Background Covariance Matrix
CP-AO	yes	yes	coupled	coupled
CP-A	yes	no	coupled	coupled
CP-O	no	yes	coupled	coupled
As-O	yes	yes	1st: atmos. model (forced by SST obs.), 2nd: ocean model (forced by atmos. analysis.)	atmos.-alone ocean-alone
CP-ABOB	yes	yes	coupled	atmos.-alone, ocean-alone
CP-A2OB	yes	yes	coupled	In CP-ABOB, add atmospheric covariance to ocean for oceanic analysis
CP-O2AB	yes	yes	coupled	In CP-ABOB, add oceanic covariance to the atmosphere for atmospheric analysis

567

568

569 **Figure Captions**

570

571 Figure 1. Time series of (a) SST ( $T$ ) and ocean thermocline depth ( $h$ ), (b) atmospheric  
 572 winds ( $x_1, x_2, x_3$ ) and air temperature ( $T_a$ ) in the control simulation of the mid-latitude  
 573 coupled system.

574

575 Figure 2. Auto correlations (solid) and cross-correlations (dash) of monthly SST, air  
 576 temperature and wind in (a) CCSM3.5 North Atlantic average and (b) the mid-latitude  
 577 coupled system. The wind is the zonal surface wind in (a) and  $x_2$  in (b). The cross-  
 578 correlations are between SST and the atmospheric temperature and wind, with the  
 579 positive lags for SST leading the atmosphere.

580

581 Figure 3. Same as Fig.1 but for the tropical coupled system.

582

583 Figure 4. Same as Fig.2 but for the tropical coupled system.

584

585 Figure 5. Analysis RMSE (normalized by the standard deviation of the control run) of all  
 586 the 6 variables for different assimilation schemes in the mid-latitude coupled system: OB:  
 587 Observation, coupled schemes CP-A, CP-O, CP-AO (CP-AO and CP-A almost overlap  
 588 with each other) and the uncoupled scheme As-O (see Table 1). The observational time  
 589 steps for the atmosphere and ocean are 10 and 40 steps, respectively. The RMSE is  
 590 calculated as the average of the RMSEs at all the analysis steps.

591

592 Figure 6. The ratio of RMSE (accumulated for all time steps) between CP-A and CP-AO  
 593 as a function of the time steps of atmospheric observation in the mid-latitude system. (a)  
 594 SST and thermocline depth, (b) air temperature. The oceanic observation time step is  
 595 fixed at 40 steps. (The ratio of RMSE at the analysis steps are similar).

596

597 Figure 7. Analysis RMSE (normalized by the standard deviation of the control run) for  
 598 As-O (circle), CP-AO (solid dot), CP-ABOB (cross), CP-A2OB (triangle) and CP-O2AB  
 599 (plus) in the mid-latitude coupled system for  $h$ ,  $T$ ,  $x_2$  and  $T_a$ . An ensemble of 80 members  
 600 is performed with the ensemble mean in marks and the ensemble spread (standard  
 601 deviation) in double bars. The observational time steps for the atmosphere and ocean are  
 602 10 and 40 steps, respectively.

603

604 Figure 8. Same as Fig.5 but for the tropical system.

605

606 Figure 9. Same as Fig.6 but for the tropical system.

607

608 Figure 10. Same as Fig.7 but for the tropical system.

609

610 Figure 11: Forecast RMSE in the mid-latitude system for  $h$  (left) and  $T$  (right) initialized  
 611 in PO (dash) and CP-AO (solid) schemes.

612

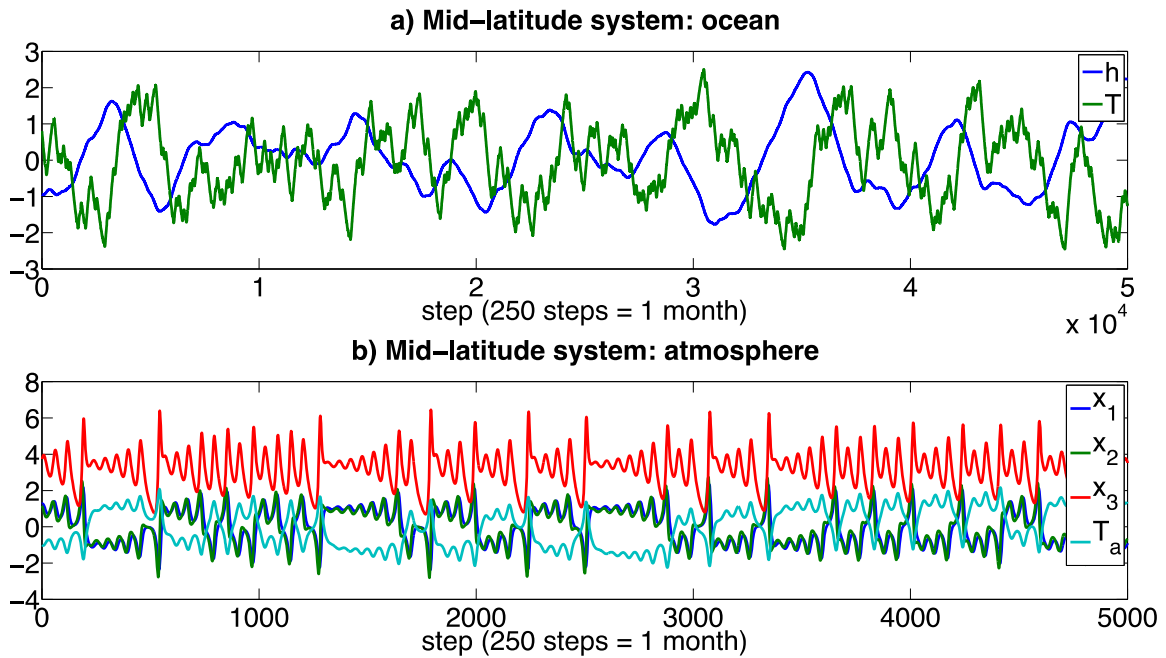
613 Figure A1. Lagged correlations among all model variables in the mid-latitude system.  
 614 Each panel represents the pivotal variable that is used for lagged correlation with itself

615 (auto-correlation) and other 5 variables (cross-correlations). The positive lead step is for  
616 this pivotal variable leading other variables. Each variable is represented in the same  
617 color, blue for  $h$ , green for  $T$ , red for  $x_1$ , cyan for  $x_2$ , purple for  $x_3$  and yellow for  $T_a$ . For  
618 example, in panel (b), the auto-correlation of T is in blue, the cross-correlation between T  
619 and  $h$ ,  $x_1$ ,  $x_2$ ,  $x_3$  and  $T_a$  are in blue, red, cyan, purple and yellow, respectively.

620

621 Figure A2. Same as Fig.A1 but for the tropical system.

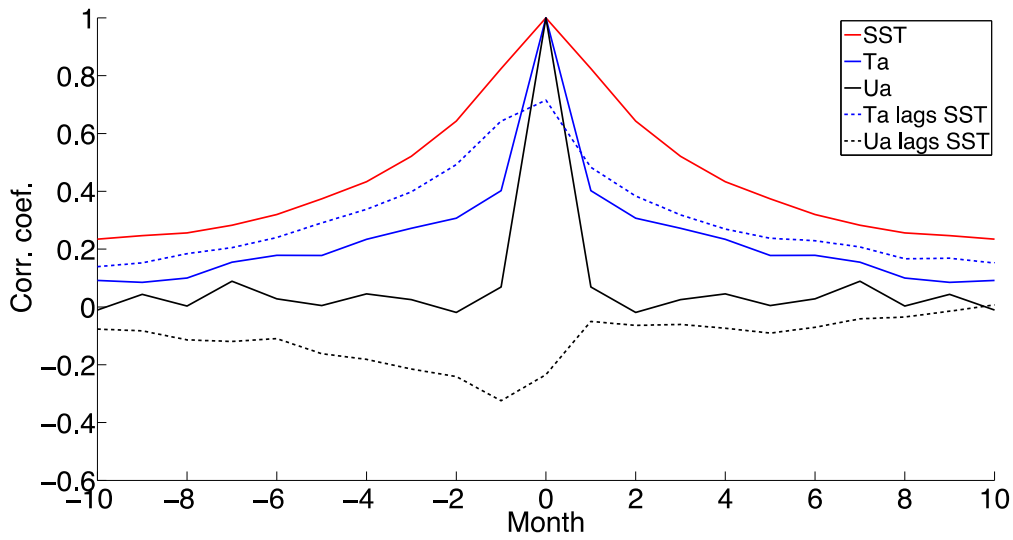
622  
623



624  
625  
626  
627  
628  
629  
630  
631  
632  
633  
634  
635  
636  
637  
638  
639  
640

Figure 1. Time series of (a) SST ( $T$ ) and ocean thermocline depth ( $h$ ), (b) atmospheric winds ( $x_1, x_2, x_3$ ) and air temperature ( $T_a$ ) in the control simulation of the mid-latitude coupled system.

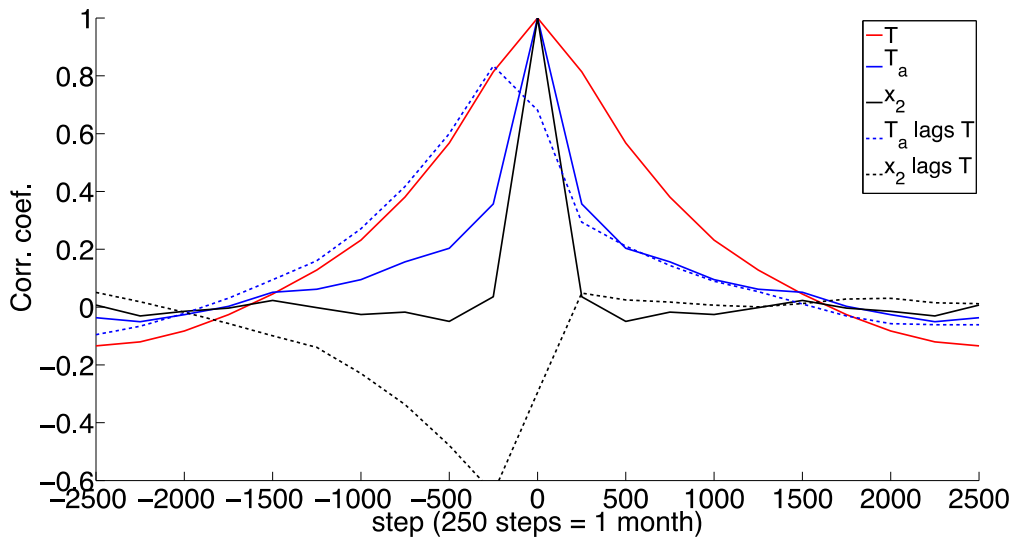
641



642

643

644



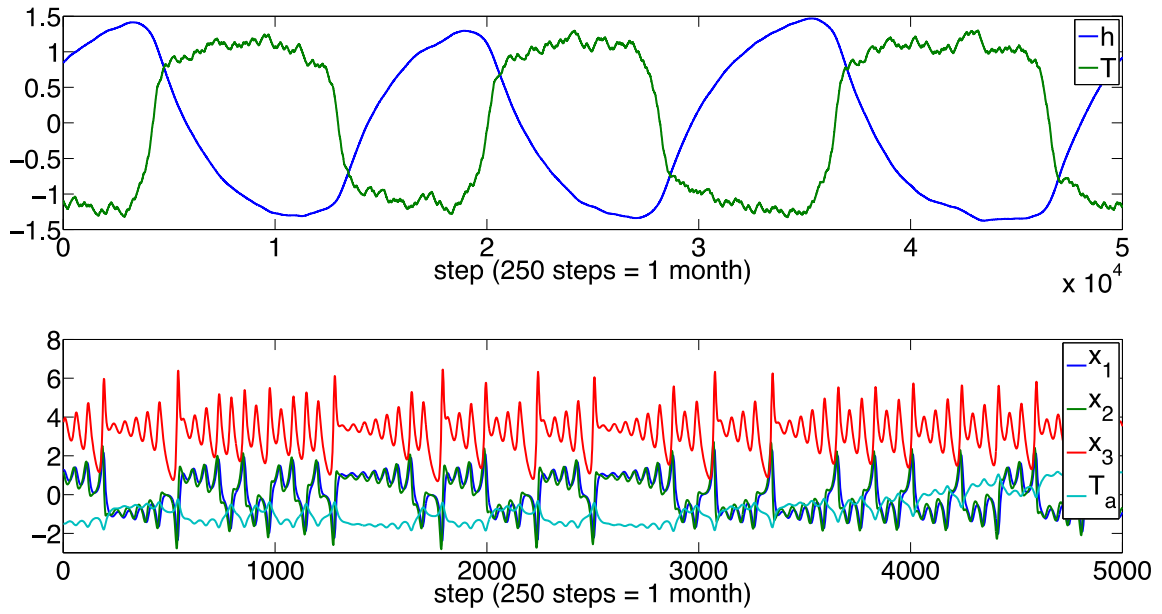
645

646

647

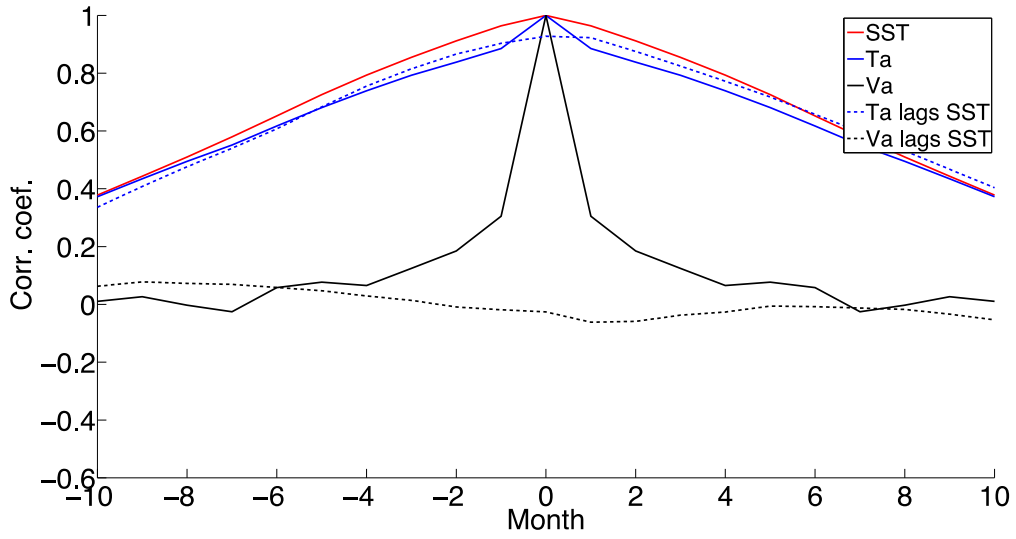
648 Figure 2. Auto correlations (solid) and cross-correlations (dash) of monthly SST, air  
 649 temperature and wind in (a) CCSM3.5 North Atlantic average and (b) the mid-latitude  
 650 coupled system. The wind is the zonal surface wind in (a) and  $x_2$  in (b). The cross-  
 651 correlations are between SST and the atmospheric temperature and wind, with the  
 652 positive lags for SST leading the atmosphere.

653  
654

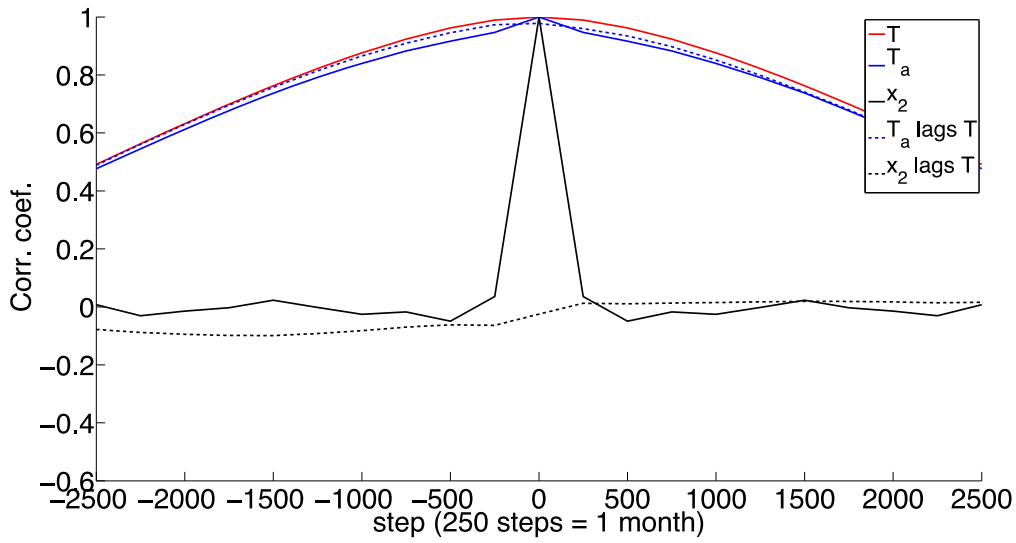


655  
656  
657  
658  
659  
660

Figure 3. Same as Fig.1 but for the tropical coupled system.



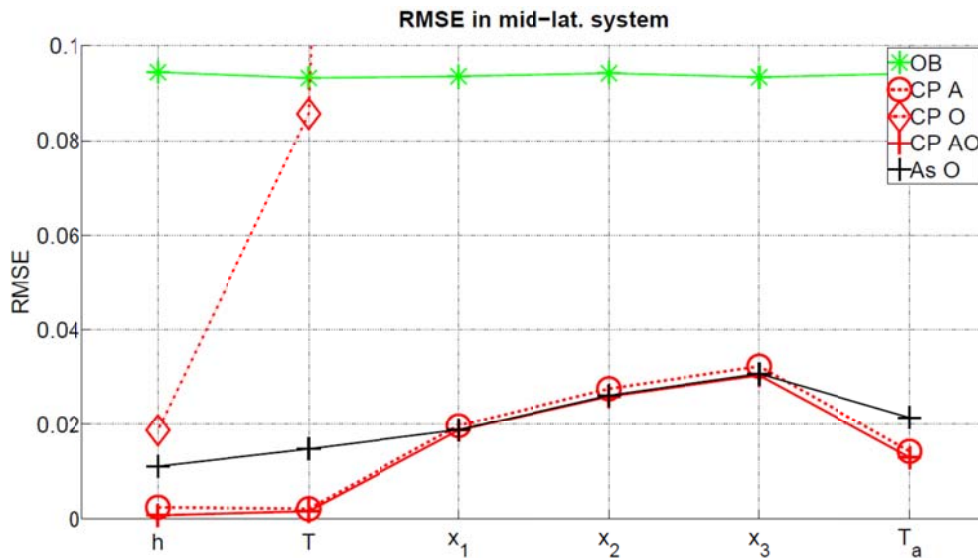
661  
662  
663



664  
665  
666  
667  
668  
669  
670  
671

Figure 4. Same as Fig.2 but for the tropical coupled system.

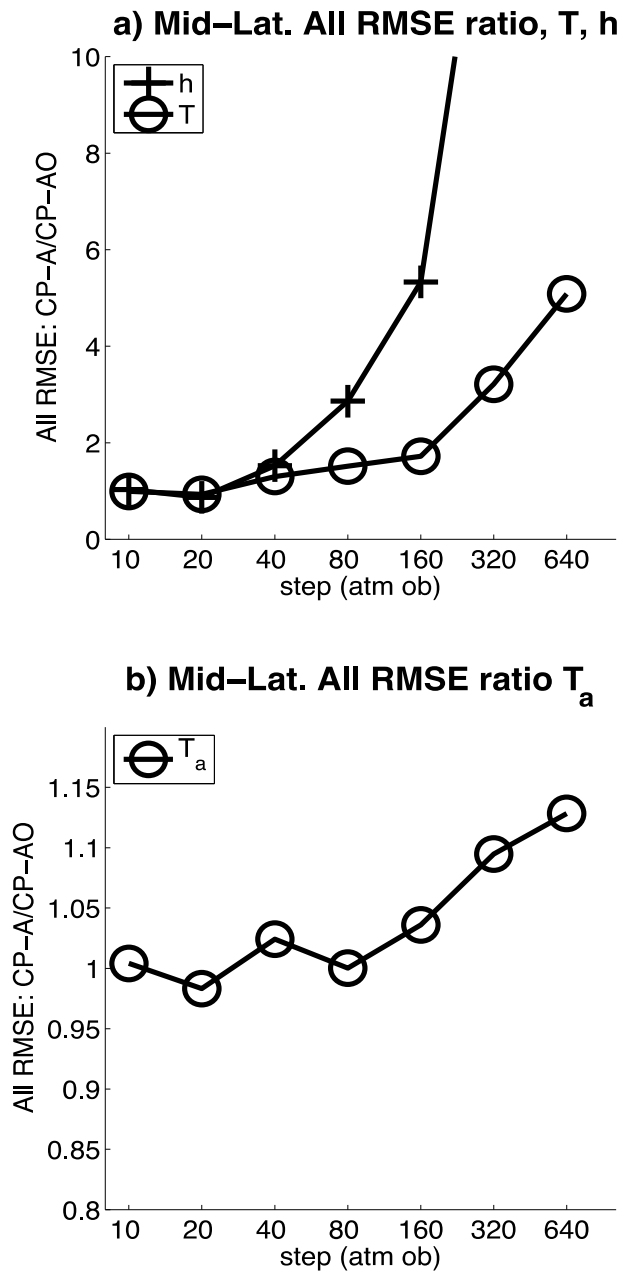
673  
674  
675  
676  
677  
678  
679  
680



681  
682  
683  
684  
685  
691  
692  
693  
694  
695  
696  
697

Figure 5. Analysis RMSE (normalized by the standard deviation of the control run) of all the 6 variables for different assimilation schemes in the mid-latitude coupled system: OB: Observation, coupled schemes CP-A, CP-O, CP-AO (CP-AO and CP-A almost overlap with each other) and the uncoupled scheme As-O (see Table 1). The observational time steps for the atmosphere and ocean are 10 and 40 steps, respectively. The RMSE is calculated as the average of the RMSEs at all the analysis steps.

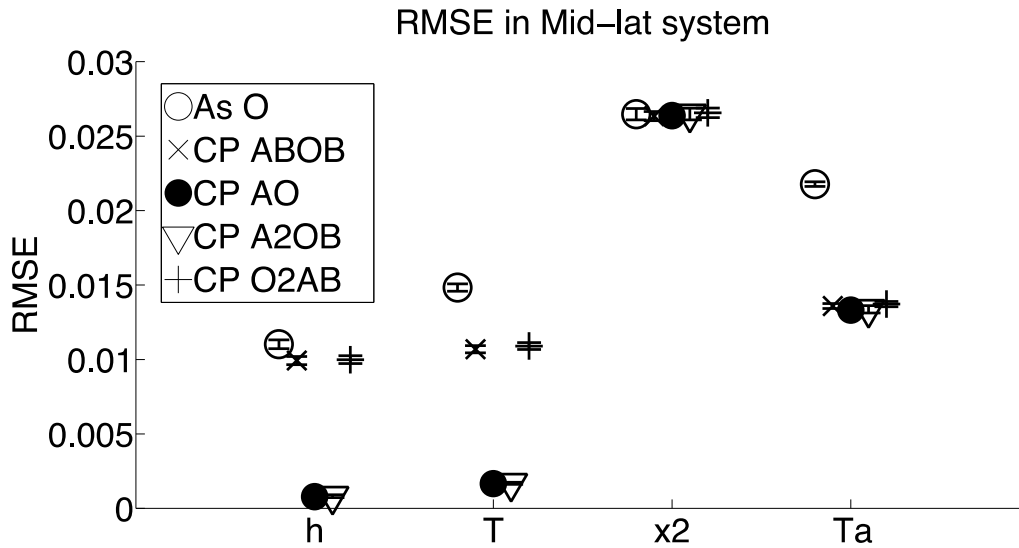
692  
693  
694



695  
696  
697  
698  
699  
700  
701  
702  
703

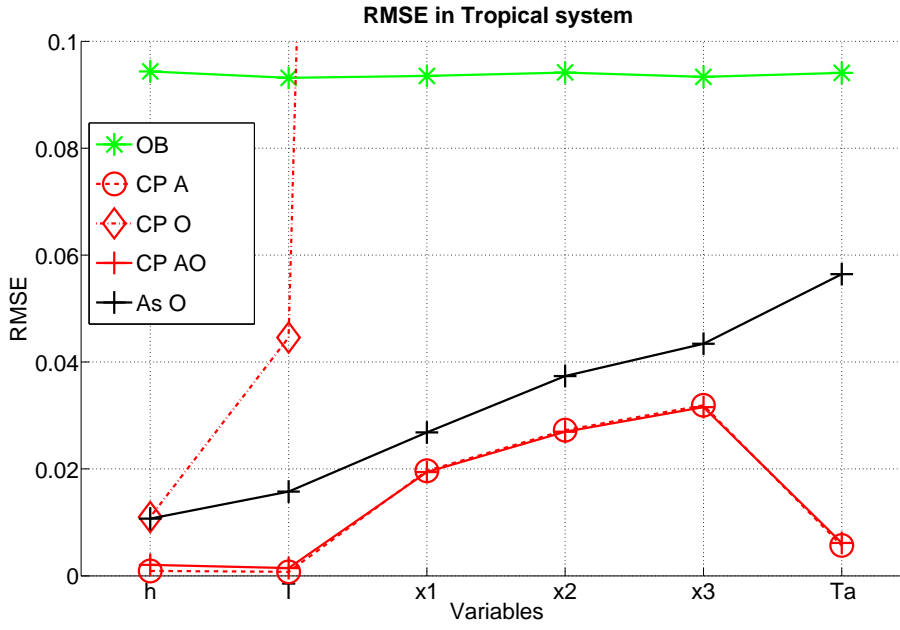
Figure 6. The ratio of RMSE (accumulated for all time steps) between CP-A and CP-AO as a function of the time steps of atmospheric observation in the mid-latitude system. (a) SST and thermocline depth, (b) air temperature. The oceanic observation time step is fixed at 40 steps. (The ratio of RMSE at the analysis steps are similar).

704



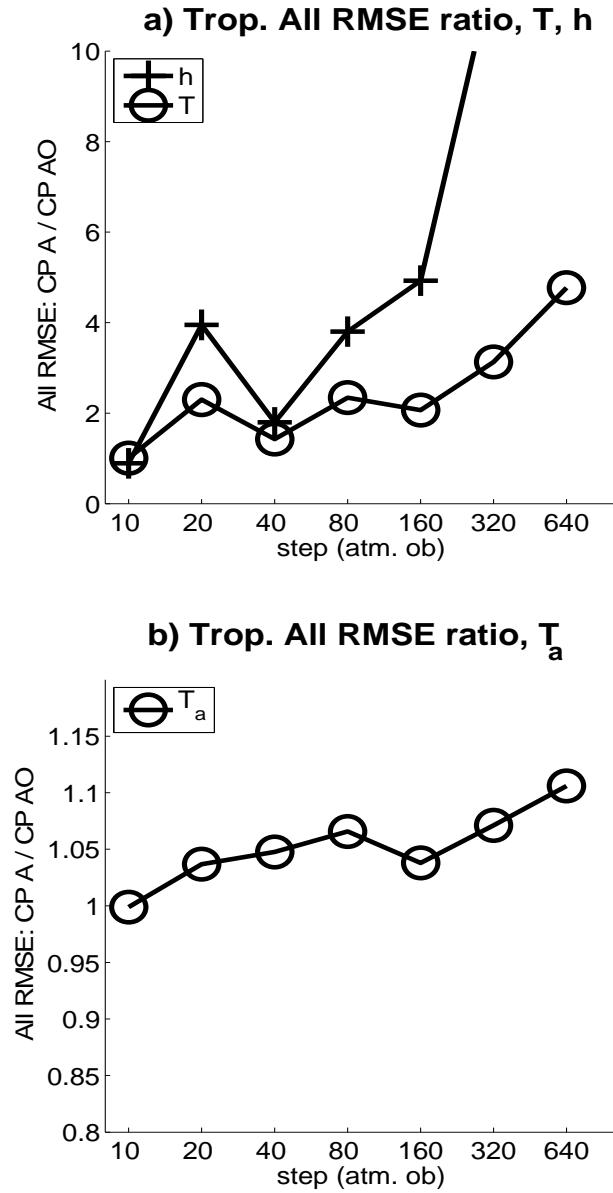
705  
 706  
 707  
 708  
 709  
 710  
 711  
 712  
 713  
 714  
 715  
 716  
 717  
 718  
 719  
 720  
 721  
 722  
 723  
 724  
 725  
 726  
 727  
 728  
 729  
 730

Figure 7. Analysis RMSE (normalized by the standard deviation of the control run) for As-O (circle), CP-AO (solid dot), CP-ABOB (cross), CP-A2OB (triangle) and CP-O2AB (plus) in the mid-latitude coupled system for  $h$ ,  $T$ ,  $x_2$  and  $T_a$ . An ensemble of 80 members is performed with the ensemble mean in marks and the ensemble spread (standard deviation) in double bars. The observational time steps for the atmosphere and ocean are 10 and 40 steps, respectively.



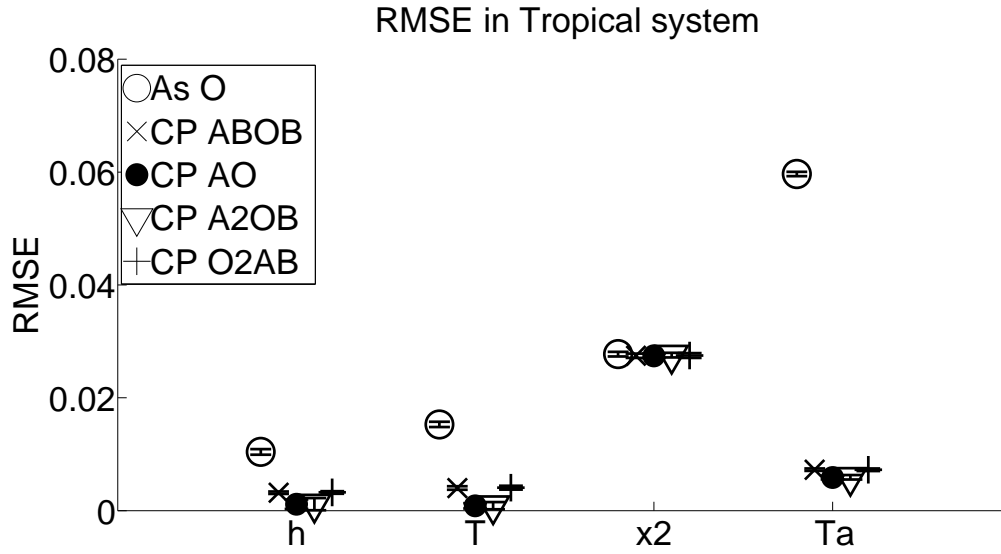
731  
 732  
 733  
 734  
 735  
 736  
 737  
 738  
 739  
 740  
 741  
 742  
 743

Figure 8. Same as Fig.5 but for the tropical system.



744  
 745  
 746  
 747  
 748  
 749  
 750  
 751  
 752  
 753  
 754  
 755  
 756  
 757  
 758

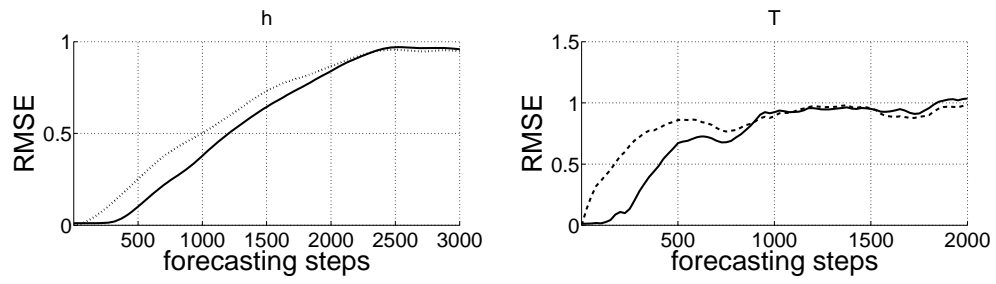
Fig.9: Same as Fig.6 but for tropical system.



759  
 760  
 761  
 762  
 763

Fig.10: Same as Fig.7 but for the tropical system.

764

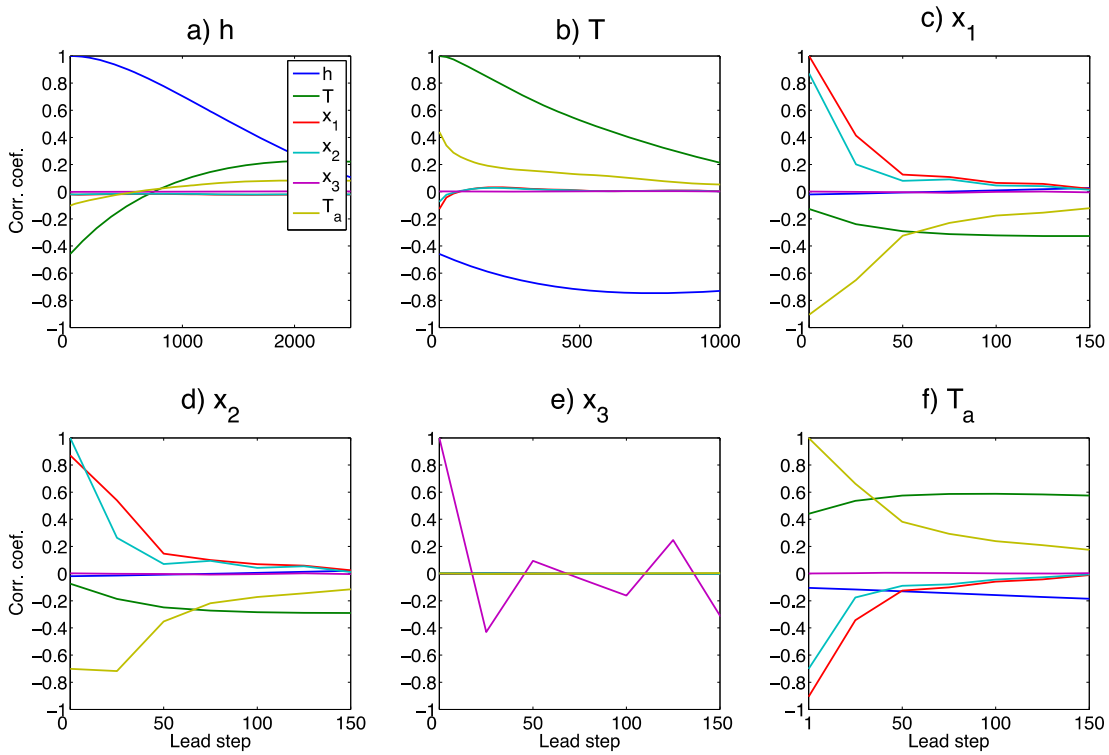


765

766 Figure 11: Forecast RMSE in the mid-latitude system for h (left) and T (right) initialized  
767 in PO (dash) and CP-AO (solid) schemes.

768

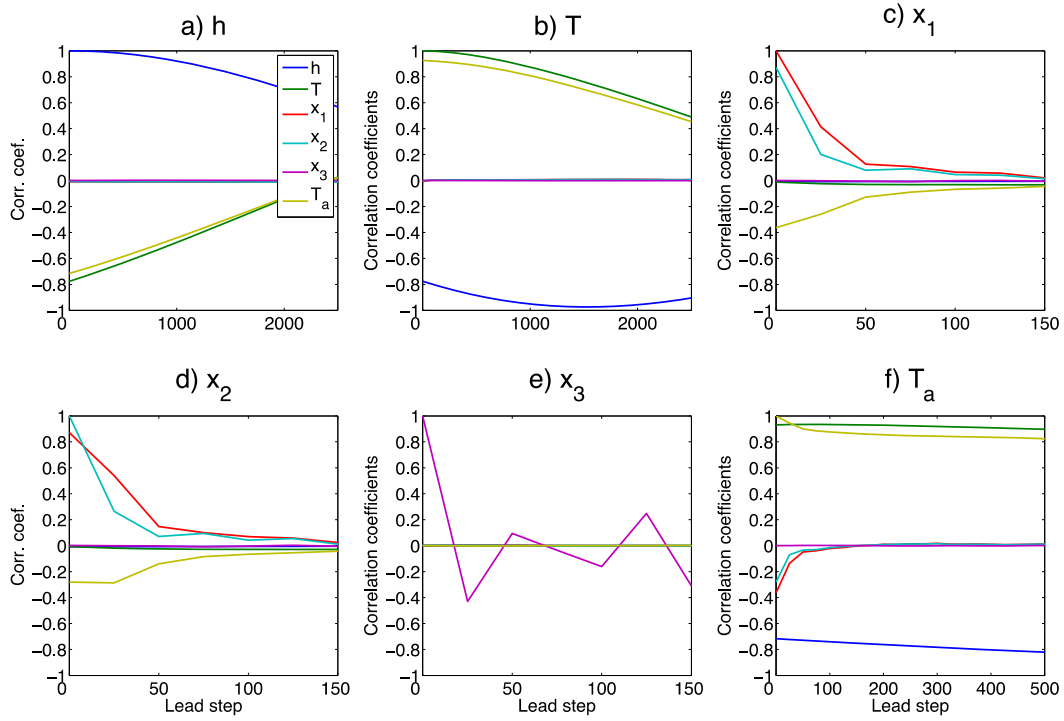
769  
770



771  
772  
773  
774  
775  
776  
777  
778  
779  
780  
781  
782

Figure A1. Lagged correlations among all model variables in the mid-latitude system. Each panel represents the pivotal variable that is used for lagged correlation with itself (auto-correlation) and other 5 variables (cross-correlations). The positive lead step is for this pivotal variable leading other variables. Each variable is represented in the same color, blue for  $h$ , green for  $T$ , red for  $x_1$ , cyan for  $x_2$ , purple for  $x_3$  and yellow for  $T_a$ . For example, in panel (b), the auto-correlation of  $T$  is in blue, the cross-correlation between  $T$  and  $h$ ,  $x_1$ ,  $x_2$ ,  $x_3$  and  $T_a$  are in blue, red, cyan, purple and yellow, respectively.

783



784  
785  
786  
787

Figure A2. Same as Fig.A1 but for the tropical system.